HHS Public Access

Author manuscript

Nat Plants. Author manuscript; available in PMC 2019 March 24.

Published in final edited form as:

Nat Plants. 2018 October ; 4(10): 824–835. doi:10.1038/s41477-018-0253-3.

Molecular basis of flowering under natural long-day conditions in *Arabidopsis*

Young Hun Song[#1,2], **Akane Kubota**[#1], **Michael S. Kwon**[1], **Michael, F. Covington**[3], **Nayoung Lee**[1], **R. Taagen Ella**[1], **Dianne Laboy Cintrón**[1], **Dae Yeon Hwang**[2], **Reiko Akiyama**[4], **K. Hodge Sarah**[5], **He Huang**[6], **Nhu H. Nguyen**[1], **A. Nusinow Dmitri**[6], **J. Millar Andrew**[5], **Kentaro K. Shimizu**[4,7], and **Takato Imaizumi**[1]

[1]Department of Biology, University of Washington, Seattle, WA, 98195, USA. [2]Department of Life Sciences, Ajou University, Suwon, 443-749, Korea. [3]Amaryllis Nucleics, Oakland, CA, 94609, USA. [4]Department of Evolutionary Biology and Environmental Studies, University of Zürich, 8057 Zürich, Switzerland. [5]School of Biological Sciences and SynthSys, University of Edinburgh, Edinburgh, EH9 3BF, UK [6]Donald Danforth Plant Science Center, St. Louis, MO, 63132, USA. [7]Kihara Institute for Biological Research, Yokohama City University, Yokohama, Kanagawa, 244-0813, Japan

[#] These authors contributed equally to this work.

Abstract

Plants sense light and temperature changes to regulate flowering time. Here we show that expression of the *Arabidopsis* florigen gene, *FLOWERING LOCUS T* (*FT*), peaks in the morning during spring, a different pattern than we observe in the lab. Providing our lab growth conditions with a red/far-red light ratio similar to open field conditions and daily temperature oscillation is sufficient to mimic the *FT* expression and flowering time in natural long days. Under the adjusted growth conditions, key light signaling components, such as phytochrome A (phyA) and EARLY FLOWERING 3 (ELF3), play important roles in morning *FT* expression. These conditions stabilize CONSTANS (CO) protein, a major *FT* activator, in the morning, which is likely a critical mechanism for photoperiodic flowering in nature. Refining the parameters of our standard growth conditions to more precisely mimic plant responses in nature can provide a powerful method for improving our understanding of seasonal response.

Materials and Correspondence: Correspondence and requests for materials should be address to T.I (takato@uw.edu) and Y.H.S. (younghsong@ajou.ac.kr).

Author contributions: T.I. conceived the project, and Y.H.S., A.K., and T.I. designed the experiments. Y.H.S., A.K., M.S.K., M.F.C., N.L., E.R.T., D.L.C., D.Y.H., R.A., S.K.H, H.H., N.H.N, D.A.N., A.J.M., and T.I. performed experiments and analyses, Y.H.S., A.K., and T.I. wrote the manuscript with the help of R.A., D.A.N., A.J.M., and K.K.S.

Competing interests: Authors declare no competing interests.

Data availability.

All data is available in the main text or the supplementary materials. The raw sequence data (GSE110605) were deposited in NCBI Sequence Read Archive. The mass spectrometry proteomics data were deposited to the ProteomeXchange Consortium via the PRIDE partner repository with the dataset identifier PXD010518 and 10.6019/PXD010518.

Main Text:

Many plants utilize day-length (=photoperiod) and temperature information to control various seasonal responses for survival and reproduction. Among the seasonal responses, flowering regulation in *Arabidopsis* is the most characterized response at the molecular level[1]. Photoperiod and temperature information is processed through circadian clock-dependent mechanisms to induce the expression of the florigen gene, *FT*, around dusk in long days (LD)[2, 3]. This LD specific *FT* induction occurs in leaf phloem companion cells. Once synthesized in LD, FT protein is transferred from the leaves to the shoot apical meristem to trigger the transition from vegetative to reproductive development[4].

Many components in the *Arabidopsis* photoperiodic pathway are highly conserved in angiosperms (including major crops such as rice, wheat, barley, and potato) to regulate seasonal responses. For instance, genes identified through quantitative trait locus (QTL) analyses on flowering time, yield, or other domestication traits (often tied with loss/reduction of photoperiod sensitivity) in many crops frequently turned out to be homologs of the *Arabidopsis* photoperiodic flowering components[5]. The photoperiodic sensing mechanism originally characterized in *Arabidopsis* was found to already exist in bryophytes to regulate photoperiodic reproductive development[6]. This indicates that incorporating photoperiodic information into developmental regulation has been important for land plant survival.

Thus far, *Arabidopsis* research has been instrumental in not only identifying the components involved in photoperiodic flowering, but also understanding how these components function in this pathway under well-controlled lab settings. However, it remains unknown whether the current model of photoperiodic flowering regulation can recapitulate the seasonal flowering mechanisms in complicated natural LD environments. Here we show the presence of a previously uncharacterized regulation of florigen induction in *Arabidopsis* plants grown in natural LD, and our subsequent attempt to elucidate its regulatory mechanism using lab growth conditions optimized to plant responses in nature.

Results

Flowering regulation under natural LD conditions

Light (day length and light quality) and temperature are major environmental parameters that control flowering time[2, 3, 7]. The day length and temperature conditions of the summer solstice in Seattle, WA, USA, (47°36′N; day length, 15 hours 59 min; average high temperature from 1971 to 2000, 21.1 °C) were similar to our lab LD conditions (16 hours, constant 22 °C). In addition, ecological studies showed that summer annuals of wild *Arabidopsis* plants grown in similar latitudes to Seattle germinate and flower within a roughly one month period between March and July in both Europe and North America[8, 9, 10, 11, 12, 13, 14, 15]. Therefore, we tested how accurately photoperiodic flowering regulation that occurs in controlled lab environments can represent flowering regulation under similar natural LD conditions.

We grew wild-type (WT: Col-0) plants outside in Seattle in June and harvested them around the summer solstice (Fig. 1a and Supplementary Fig. 1). We analyzed the expression of genes important for photoperiodic flowering regulation (Fig. 1b, c and Supplementary Fig. 2)[3]. The expression patterns of six circadian clock genes, clock output flowering genes, and floral repressor genes were relatively similar to those already described in the lab-grown samples (Supplementary Fig. 2)[16, 17, 18, 19]. In addition, the night-peaking *CO* expression profile was similar to the one in lab LD with cooler nights (Fig. 1b)[19]. These results indicate that simplified lab conditions recapitulate the natural gene expression profiles of those genes. However, in the plants grown outside, *FT* showed a bimodal expression pattern with peaks in the morning and around dusk (Fig. 1c), which clearly differed from the typical *FT* pattern peaking near dusk in lab LD[17, 20]. We also observed a similar bimodal expression pattern in *TWIN SISTER OF FT* (*TSF*), a related florigen gene (Supplementary Fig. 2l)[20].

Since *FT* levels strongly correlate with flowering time[19, 21], we analyzed the flowering time of Col-0 plants grown in natural LD. During the last five years, even though temperatures around the summer solstice varied (Supplementary Fig. 1), Col-0 plants all flowered at similar developmental times with fewer leaves than plants grown in lab LD (Fig. 1d). In addition, we repeatedly observed similar *CO* and *FT* expression patterns in samples harvested around the last five summer solstices (Fig. 1b, c, e-g and Supplementary Fig. 3 and 5). We also grew other accessions, such as a common lab accession, L*er,* and another WT accession, Vancouver-0 (Van-0, isolated from Vancouver, BC, Canada; 49°15′N) in natural LD. We speculated that Van-0 is adapted to an environment similar to Seattle. Both accessions flowered earlier than Col-0 in lab LD, even slightly earlier in natural LD (Fig. 1d), and showed bimodal *FT* expression patterns in natural LD (Supplementary Fig. 4).

We also analyzed the phenotypes of some non-transgenic alleles of photoperiodic flowering mutants, such as *flavin-binding, kelch repeat, f-box 1 (fkf1*) and *gigantea* (*gi-2*), in natural LD. The flowering time of these late-flowering mutants was significantly earlier than that in lab LD (Fig. 1d). The *fkf1* mutant flowered at almost the same time as Col-0 plants in natural LD, suggesting that some regulation that takes place outside but not in the lab may trigger earlier flowering in the *fkf1* mutant. When we analyzed *FT* expression patterns in *fkf1* and *gi-2* grown in natural LD, the *gi-2* mutant lost *FT* expression as expected[22], but the morning *FT* expression was clearly observed in *fkf1* (Fig. 1e). These results suggest that morning *FT* expression in *fkf1* is likely the cause of the early flowering phenotype of *fkf1* in natural LD.

As our results suggested a functional contribution of morning *FT* expression on flowering in natural LD, we analyzed the expression patterns of *FT* in samples grown in different times in spring (April, May, and June), which is the growth season of summer annuals[8, 9, 10, 11, 12, 14]. In Seattle, the days are already lengthening in April (approximately 14 hours); however, the ambient temperature in April was colder than in May and June (Supplementary Fig. 1). Col-0 plants flowered later in April than in May and June (Fig. 1h). In all samples grown during spring in the last two years, *FT* peaked in the morning with different levels (lower in April than in May and June) without changing *CO* patterns (Fig. 1f and Supplementary Fig. 5).

Next, we tested whether the *FT* morning peak is observed in two native locations of *Arabidopsis*. We grew Col-0 plants in Zürich (47°37'N, similar latitude to Seattle), and in Edinburgh, (55°57'N) in June. Although the temperatures (and day length in Edinburgh) were different than in Seattle (Supplementary Fig. 6), Col-0 plants grown in both locations flowered at a similar developmental timing to the ones grown in Seattle (Fig. 1h). Both samples also showed the morning expression of *FT*, although the afternoon *FT* expression levels differed (Fig. 1g and Supplementary Fig. 7). These results indicate that WT plants grown in natural LD induce *FT* in the morning and possibly around dusk to induce early flowering.

Reconstitution of lab growth conditions that reflect natural conditions for flowering

Our results obtained from plants grown in natural LD demonstrated that our current lab LD conditions are not sufficient to reproduce all important flowering regulation. To more precisely study these mechanisms, we adjusted our current growth conditions using *FT* expression patterns as a proxy for the flowering regulation in nature. We first hypothesized that the daily light intensity changes might alter the *FT* pattern, compared to step changes (=light on/off) under lab conditions. The light intensity changes did not drastically alter the *FT* pattern (or *CO* and *TSF*) (Supplementary Fig. 8a-e), indicating that light on/off conditions might be sufficient. Daily temperature changes affect *FT* expression patterns[19, 23]. Therefore, we analyzed the effect of daily temperature fluctuation on *FT* expression. When Col-0 plants were grown in lab LD with daily temperature oscillations based on the average changes that occurred around the summer solstice (Supplementary Fig. 8f, g), *CO* was strongly induced at the end of the night (Supplementary Fig. 8h). The afternoon *FT* levels (but not the *TSF* levels) were severely repressed by daily temperature changes (Supplementary Fig. 8i, j). These results suggest that temperature oscillation is not enough to induce *FT* in the morning, although it can repress *FT* in the afternoon.

The red to far-red (R/FR) ratio in an open field (including our outside conditions) is approximately 1 (ref [24]), but it varies from approximately 2 (our lab conditions) to 13 (ref [24]) under fluorescent lamps. Plant shade conditions (=very low R/FR ratios) highly induce the *FT* expression even in the morning[25, 26]. We wondered whether the morning *FT* expression could be induced under R/FR ratio=1 conditions. To test this, we supplemented our fluorescent lamps (R/FR=2) with dim FR LEDs to adjust the R/FR ratio to 1 (Supplementary Fig. 9a). Merely adjusting the R/FR ratio from 2 to 1 was sufficient to induce *FT* (and *TSF*) in the morning, without affecting *CO* expression patterns (Fig. 2a and Supplementary Fig. 9b, c). Under these conditions (named LD+FR), the levels of both morning and afternoon *FT* levels were higher than in lab LD (Fig. 2a). However, the afternoon *FT* peak was still slightly higher than the morning peak, different from the *FT* patterns in natural LD. We also tested whether R/FR=1 induces *FT* in the morning independent of photoperiod changes. We analyzed *FT* expression in short days (SD) with R/FR=1 (SD+FR). *FT* was not induced in SD+FR, similar to regular SD (Supplementary Fig. 10), implying that the morning induction of *FT* under LD+FR conditions is long-day specific.

As temperature oscillation reduced afternoon *FT* levels (Supplementary Fig. 8i), we hypothesized that combining the R/FR=1 conditions with daily temperature changes may cause a similar *FT* pattern to that observed outside. Incorporating these two parameters in the simplified lab conditions (LD+FR+temp) was sufficient to generate similar *FT* expression patterns (and *CO* and *TSF*) to that observed in nature (Fig. 2b and Supplementary Fig. 11). We then analyzed the flowering time of WT accessions and photoperiodic mutants including *co*, *ft*, *ft tsf* and *fkf1* under the LD+FR+temp conditions. WT plants and *fkf1* alleles (*fkf1* and *fkf1–2*) flowered earlier in LD+FR+temp than in lab LD (Fig. 2c). In addition, the *FT* expression profile in *fkf1–2* was similar to that in *fkf1* grown in natural LD (Supplementary Fig. 12), validating that the simplified LD+FR+temp conditions captured the major environmental parameters to recreate the *FT* expression patterns and flowering time responses of the plants grown in natural LD. Importantly, the *co*, *ft* single and *ft tsf* double mutants still showed a similar late flowering phenotype under all experimental conditions (Fig. 2c). In addition, the *ft-1 tsf-1* double mutants flowered later than the *ft-1* mutant (Fig. 2c), indicating that changes in the expression patterns of both *FT* and *TSF* may contribute to flowering time in LD+FR+temp.

We also analyzed whether the LD+FR+temp conditions changed the spatial expression patterns of *FT* to induce its morning peak. The tissue-specific GUS activity patterns in the *FT:GUS* plants were similar in LD, LD+FR, and LD+FR+temp (Fig. 2d and Supplementary Fig. 13), indicating that the adjustment of the R/FR ratio and temperature mainly affected the temporal expression pattern of *FT*.

To explore the similarities between LD+FR+temp and natural LD conditions on a whole transcriptome scale, we performed RNA-sequencing analysis using WT plants grown in lab LD, LD+FR+temp, and two years (2013 and 2014) of natural LD conditions. The samples were harvested at Zeitgeber time 4 (ZT: time after light onset) when morning *FT* peaks. Compared with lab LD conditions, 57 genes were consistently upregulated in the morning in two different years of natural LD and LD+FR+temp conditions (Fig. 3a and Supplementary Table 1). GO term enrichment analysis showed that genes involved in light (UV-B, FR, and R) responses were enriched (Fig. 3a and Supplementary Table 1). Among these 57 genes, only four, including *FT* and *TSF*, were identified as flowering genes, based on FLOR-ID[27] (Fig. 3b). In the downregulated genes common among the three conditions compared with the lab LD condition, environmental stress-related genes were enriched (Supplementary Fig. 14 and Supplementary Table 1). However, there were no downregulated flowering genes overlapping among the three conditions (Supplementary Fig. 14). These results indicate that *FT* and *TSF* induction levels might be the major difference important for flowering time regulation between LD and LD+FR+temp as well as natural LD conditions.

Flowering time is a critical adaptive trait within WT accessions[28]. Our data showed that the generation of the *FT* morning peak was closely related to the early flowering phenotypes in natural LD (Fig. 1c-h). We asked whether this mechanism is widely conserved in WT accessions. To test this, we compared *FT* levels between morning and evening among 20 summer annual accessions[29] originating from different latitudes (Supplementary Fig. 15a) grown in lab LD and LD+FR+temp. In LD, *FT* levels in all accessions were significantly higher in the afternoon than in the morning (Fig. 3c and Supplementary Fig. 15b). However,

in LD+FR+temp, the differences in *FT* levels between morning and evening were much reduced (Fig. 3c and Supplementary Fig. 15c). These results suggest that the mechanisms that induce morning *FT* expression in LD+FR+temp are largely conserved across *Arabidopsis* accessions.

Components important for flowering time regulation in nature

As our LD+FR+temp conditions reproduced *FT* expression profiles similar to those in natural LD (Fig. 2b), we next investigated whether any known components in the flowering and light signaling pathways are involved in the regulation of morning *FT* expression. Because CO is a chief activator of *FT*[1], we first analyzed *FT* expression in the *co* mutant. *FT* levels in the *co* mutant were very low throughout the day in LD+FR+temp, LD, and LD+FR (Fig. 4a-c), implying that CO function is essential for *FT* induction even under conditions more similar to the natural environment. We then analyzed *FT* expression patterns in photoreceptor and light signaling mutants, circadian clock mutants, and mutants in the ambient temperature flowering pathway in LD+FR+temp (Fig. 4a-f and Supplementary Fig. 16)[1, 3, 30]. Compared with WT plants, *FT* expression in the morning was specifically reduced in the *phytochrome A* (*phyA*) mutant (*phyA-211*) in LD+FR+temp (Fig. 4a). This phenotype was also pronounced in LD+FR (Fig. 4b, c). These results prompted us to analyze the flowering phenotype of the *phyA* mutant in natural LD and LD+FR+temp conditions. To grow the *phyA* mutant outside, we utilized non-transgenic *phyA-201* allele (L*er* background), since *phyA-211* possesses a transgene[31]. *phyA-201* flowered later than L*er* plants outside (Supplementary Fig. 17a). Previous studies posited that a certain amount of FR light is required to observe phyA-dependent effects on flowering, as *phyA* mutants only showed a late flowering phenotype in LD with lower R/FR ratio in the afternoon or in continuous FR light conditions[7, 32]. In LD+FR+temp conditions, both *phyA-201* and *phyA-211* flowered later than their parental accessions (Supplementary Fig. 17a). These results indicate that both natural LD and LD+FR+temp conditions (R/FR=1) contain enough FR light to observe the phyA contribution to flowering induction. We also analyzed *FT* expression in *phyA-201*, and found that *FT* levels were lower in both morning and afternoon than L*er* plants (Supplementary Fig. 17b, c). This result indicates that, although phyA is clearly involved in *FT* induction in the morning, its contribution to afternoon *FT* expression may differ in either different backgrounds and/or alleles. We further assessed the significance of the phyA signaling using the *far-red elongated hypocotyl 1* (*fhy1*) *fhy1-like* (*fhl*) mutant (Col-0 background) in which phyA signaling is severely attenuated due to impairment of phyA nuclear transport[33]. Although the phenotype was weaker than the *phyA-211* mutant, *fhy1 fhl* also showed a reduction in morning *FT* expression in LD+FR +temp (Supplementary Fig. 16a, b). This result further supports the notion that phyA signaling is involved in flowering regulation through inducing *FT* in natural LD.

phyA functionally antagonizes phyB in flowering[34, 35]. In *phyB* mutant, *FT* levels were higher than in WT plants in LD+FR+temp (Fig. 4d). In *early flowering 3* (*elf3*), which is a phenocopy of the *phyB* mutants[36], *FT* levels were even higher than in the *phyB* mutant (Fig. 4d-f). The difference between *phyB* and *elf3* mutants was more pronounced in LD and LD +FR (Fig. 4d-f). These results suggest that ELF3 may regulate not only phyB signaling but also other signaling pathways important for *FT* induction.

Despite being downstream signaling components of phyB and ELF3[37, 38], PHYTOCHROME INTERACTING FACTOR 1 (PIF1), PIF3, PIF4, and PIF5 might not be important for *FT* induction in LD+FR+temp, as *FT* profiles in the *pif1 pif3 pif4 pif5* (*pifq*) mutant resembled that in WT (Supplementary Fig. 16c, d). The *FT* levels in both *constitutive photomorphogenic 1* (*cop1*) and the *suppressor of phyA-105 1* (*spa1*) *spa3 spa4* triple mutants were higher without changing *CO* mRNA patterns (Supplementary Fig. 16c, d). As COP1 and SPAs directly control CO protein degradation[39, 40], this indicates that CO protein stability regulation is still important in LD+FR+temp. In the *cryptochrome 1* (*cry1*) *cry2* double mutant, *FT* expression occurred just in the morning (Supplementary Fig. 16e, f). This result prompted us to analyze the flowering phenotype in LD+FR+temp. The *cry1 cry2* mutant flowered significantly earlier in LD+FR+temp than in LD (Supplementary Fig. 18), which resembles the flowering phenotypes of *fkf1* mutants. This result further indicates that the morning expression of *FT* contributes to flowering time regulation.

Circadian clock components often regulate *FT* expression in LD[1]. *FT* levels were depressed in both *gi* and *pseudo response regulator7* (*prr7*) *prr9* mutants in LD+FR+temp (Supplementary Fig. 16e-h). In the *circadian clock associated 1* (*cca1*) *late elongated hypocotyl* (*lhy*) double mutant, *FT* levels during the afternoon were strongly increased in LD +FR+temp (Supplementary Fig. 16g, h). Based on these mutant phenotypes, our results suggest that *GI* and *PRR*s are important for the induction of *FT* throughout the day[22, 41], while morning clock genes, CCA1 and LHY, strongly repressed *FT* mainly in the afternoon[1, 42].

In the ambient temperature pathway mutants, such as *short vegetative phase* (*svp*), the triple mutant of *svp flowering locus m* (*flm*) *flowering locus c* (*flc*), and *high expression of osmotically responsive genes 1* (*hos1*)[29, 43], the difference in morning *FT* levels looked greater than that in the afternoon (Supplementary Fig. 16i, j). This could be due to lower temperatures in the morning, which activate the ambient temperature pathway. In summary, based on our results, several known components are involved in morning *FT* expression regulation.

To further investigate the mechanisms of morning *FT* induction, we studied possible interactions between phyA and ELF3. Our results showed that phyA functions as an *FT* activator, while ELF3 is a *FT* repressor in the morning in LD+FR+temp (Fig. 4a, d). In addition, phyA was identified as one of the proteins co-immunoprecipitated with ELF3, indicating that phyA and ELF3 may exist in the same protein complex[44]. First, as *FT* levels are highly increased under lower R/FR ratios, and *FT* levels are the major determinants of plant shade-induced flowering timing[25, 26, 45], and because the R/FR=1 condition is enough to induce *FT* in the morning, we investigated the more comprehensive relationship between R/FR ratios and *FT* levels. Also, we analyzed whether the *phyA* and *elf3* mutations affect *FT* levels in LD with different R/FR ratios. In WT plants, there is nearly a linear relationship between the decrease in the R/FR ratios and the increase in *FT* levels in the morning (ZT4) and the afternoon (ZT16) (Fig. 4g, h). In the *phyA-211* mutant, morning *FT* induction was severely reduced under a wide range of R/FR ratios, while morning *FT* levels in the *elf3–1* mutant were constantly high (Fig. 4g). In both *phyA-211* and *elf3–1* mutants, *FT* levels over different R/FR ratios stayed at nearly similar levels at ZT4 (Fig. 4g), indicating that the

function of both proteins is required to tune *FT* levels in response to R/FR ratio changes during the morning. In the afternoon, the lack of *elf3* made the plants more sensitive to the R/FR ratio changes with a large increase in *FT* expression under lower R/FR ratios (Fig. 4h). There was only a small *phyA-211* mutation effect on afternoon *FT* expression levels (Fig. 4h). These results suggest that both phyA and ELF3 have time-dependent functions in light quality-controlled *FT* level regulation.

We next studied the genetic relationship between *PHYA* and *ELF3* in this regulation. There was an intermediate level of *FT* expression in the *phyA-211 elf3–1* double mutant compared to *FT* levels in each mutant under all conditions (Supplementary Fig. 19), indicating that phyA and ELF3 function antagonistically on *FT* regulation. As a biochemical study indicated the presence of a phyA-ELF3 complex[44], we examined whether our modified LD conditions influence the amount of phyA co-immunoprecipitated with ELF3 protein. In LD, phyA protein dissociated from the ELF3 complex as soon as the light was turned on, while in both LD+FR and LD+FR+temp conditions, similar amounts of phyA were co-immunoprecipitaed with ELF3 at later time points during the morning (Supplementary Fig. 20). These results suggest that the prolonged presence of the phyA-ELF3 complex in LD +FR+temp may change the expression levels and/or activity of phyA and/or ELF3 proteins.

We also analyzed the phyA and ELF3 protein expression patterns in LD+FR+temp. The accumulation levels of phyA protein in LD+FR+temp were higher during the morning than in LD, although they eventually reached trough level by the end of the day (Fig. 4i). This is likely controlled by posttranslational regulation, since *PHYA* transcript levels under these conditions were very similar (Supplementary Fig. 21a). In contrast, the ELF3 protein levels in LD+FR+temp were lower throughout the day than in LD (Fig. 4j). The *ELF3* transcript levels in LD+FR+temp were also slightly lower than in LD (Supplementary Fig. 21b). Higher expression of *FT* at ZT4 in LD+FR+temp is consistent with the higher level of its activator phyA and lower levels of its repressor ELF3 under these conditions.

We further analyzed whether ELF3 affects phyA protein patterns or *vice versa*. In LD+FR +temp, there was no difference in *PHYA* levels between WT and the *elf3* mutant (Supplementary Fig. 22a). The phyA protein levels were slightly higher in *elf3* than in WT, although the difference was not statistically significant (Supplementary Fig. 22c). There was less ELF3 protein in *phyA* than in WT without affecting transcript levels (Supplementary Fig. 22b, d), suggesting that phyA may regulate ELF3 protein levels posttranscriptionally in LD+FR+temp. However, since ELF3 is a repressor of *FT*, the reduction of ELF3 levels in the *phyA* mutants cannot be the major cause of the reduction of *FT* levels in *phyA*. Previous work showed that ELF3 forms a complex with a large number of light signaling and circadian clock components, many of which require functional phyB to physically associate with the ELF3 complex[44]. In addition, more phyA protein was co-immunoprecipitated with ELF3 after dawn in LD+FR+temp (Supplementary Fig. 20). We therefore hypothesized that phyA may affect ELF3 function by directly modulating the interaction of ELF3 with other factors in a light/temperature-dependent manner.

To assess whether phyA influences the composition of the ELF3 complex, we harvested *ELF3:ELF3–6H3F* samples with/without the *phyA* mutation in the morning of LD+FR

+temp conditions, and identified peptides co-immunoprecipitated with ELF3 using mass spectrometry analysis. We included *ELF3:ELF3–6H3F/phyB* as a reference. When we compared our peptide list of *ELF3:ELF3–6H3F* samples with the previous ones harvested in the afternoon[44], we noticed that our list did not contain peptides from ELF3-associated circadian clock proteins (Supplementary Table 2), suggesting that ELF3 does not assemble with the same Evening Complex in the morning. We identified peptides derived from COP1 but not SPA1. phyB is still important for ELF3 complex formation in the morning. The loss of *phyA* did not seem to drastically change the composition of the ELF3 complex, although fewer peptides from COP1 and phyE were detected in the *phyA* background (Supplementary Table 2). These results indicate that phyA may affect the interaction of a small number of components in the ELF3 complex. However, these results are not sufficient to evaluate whether those changes may affect either ELF3 function or *FT* transcription in the *phyA* mutant in LD+FR+temp. Further analysis is required to elucidate the exact mechanism by which phyA and ELF3 antagonistically regulate *FT* levels in LD+FR+temp.

As *CO* is required for the *FT* morning peak (Fig. 4a), and the *cop1* and *spa* triple mutants showed increased *FT* levels in LD+FR+temp (Supplementary Fig. 16c, d), we hypothesized that CO protein levels may increase under these conditions. To test this, we analyzed the diurnal expression profile of CO protein in *CO:HA-CO* plants[46] in LD and LD+FR+temp. The overall accumulation patterns of CO protein in LD and LD+FR+temp were similar (Fig. 5a). However, CO protein increased more in LD+FR+temp than in LD at the ZT4 time point, when the *FT* morning peak was induced (Fig. 5a). Therefore, we analyzed a fine scale time course of CO profiles during the morning. In LD, CO protein acutely accumulated just after dawn (ZT0.5–1) but quickly degraded by ZT2 (Fig. 5b). In LD+FR+temp, CO protein levels kept increasing until ZT1, and then decreased more gradually during the morning. The levels of CO protein expressed in the morning of LD+FR+temp was similar to the levels around dusk (Fig. 5a, b), suggesting that the elevation of CO protein levels in LD+FR+temp might contribute to morning *FT* peak generation.

CO protein levels are controlled by several E3 ubiquitin ligases, such as the COP1/SPA complex[39, 40]. Both phyA and ELF3 physically interact with the COP1/SPA1 complex to regulate its function[44, 47, 48]. We therefore investigated whether phyA and/or ELF3 mediate *FT* regulation through regulation of CO protein stability. We found that ELF3 is in the same CO protein complex *in planta* and *in vivo* (Fig. 5c and Supplementary Fig. 23). In addition, *FT* expression and the early flowering phenotype of *elf3–1* were largely dependent on functional *CO,* as *FT* expression levels are very low in both *co-101* and *elf3–1 co-101*, and *elf3–1 co-101* flowered just slightly earlier than the late flowering *co-101* mutant (Supplementary Fig. 24). Although the *FT* levels in the *elf3–1 co-101* mutant are similar to those in the previously characterized *elf3–1 co-1* mutant[49], the *elf3–1 co-1* mutant showed an intermediate flowering phenotype between the *co-1* and *elf3–1* mutants[49]. This flowering time difference might be caused by the difference in the genetic backgrounds (*elf3–1 co-1* in F3 segregants between Col-0 and Landsberg[49] cross, vs. *elf3–1 co-101* in Col-0) and/or *co* alleles. We next analyzed whether ELF3 influences CO stability, and found that CO protein was more abundant in the *elf3* mutant, including at ZT4 (Fig. 5d and Supplementary Fig. 25). Together with our results that showed lower levels of ELF3 protein in LD+FR+temp, these results indicate that ELF3 may negatively influence CO stability in the morning, and

that LD+FR+temp conditions in part reduce the amount of the negative regulator to increase CO protein stability, consistent with increased expression of its target *FT*.

Discussion

Our results indicate that the difference in R/FR ratios and daily temperature are the main causes of the difference in flowering time between natural LD and lab LD conditions. Mechanistically, this difference in growth conditions likely causes different expression levels of the florigen genes, *FT* and *TSF,* especially in the morning. Previous work indicated that *FT* induced between ZT12 and ZT20 in SD was more effective for floral induction than *FT* induced during other time windows[21]. How does morning-expressed *FT* affect flowering compared to evening-expressed? The uploading of FT proteins into the phloem and the unloading of them into the shoot apical meristem are actively regulated, at least in cucurbit plants[50, 51]. Phloem flux and the concentration of major transport sugars in phloem sap exhibit diurnal and developmental changes in some plants[52, 53, 54]. Therefore, the efficiency of florigen movement may change depending on growth conditions, time of day, and plant age. Although it is beyond the scope of our current research, it would be of interest to assess whether the timing of *FT* expression during the morning has some mechanical advantages compared to evening in natural LD.

Our results indicate that phyA and ELF3 are involved in the regulation of the morning expression of *FT* in natural LD (Fig. 5e, f). In addition, CO protein is likely more stable in the morning of natural LD than in regular lab LD. This may contribute to higher induction of *FT* in the morning. However, as CO protein interacts with several other transcription factors to regulate *FT* in the morning[55], we assume that there are still other factors that participate in controlling *FT* levels in natural LD morning (Fig. 5e, f). We therefore think the findings presented here are a starting point to understanding the mechanisms of the previously uncharacterized florigen induction that takes place in natural LD.

With the external coincidence model for explaining photoperiodic response as a basis[56], molecular mechanisms that consist of complex interplay between light signaling and the circadian clock have been proposed to explain LD specific dusk *FT* expression[1]. Although our results indicate the involvement of some known flowering regulators in morning *FT* induction, the current model cannot explain how these factors induce *FT* in the morning in natural LD. Investigating these mechanisms will help us to understand how *Arabidopsis* plants flower in spring in nature.

Behavioral rhythms in model animals (*Drosophila*, mouse, and golden hamster) differed between natural and lab conditions[57, 58, 59]. In *Drosophila*, transcriptional levels of clock genes were altered between these two conditions[60]. Even for *Arabidopsis*, previous work reported discrepancies in predicted flowering phenotypes when flowering mutants were grown outside[13], although the molecular mechanism that caused this was unknown. Based on our work, the discrepancies might be partly caused by the difference in light quality and temperature between lab and natural conditions. To understand plant response at molecular levels in nature, recent functional genomic approaches in molecular ecology have successfully revealed certain mechanisms by which plants sense specific environmental

stimuli in complex natural environments[61, 62]. However, these approaches still have geographical and environmental limitations. Our approach for optimizing simplified lab conditions based on plant response in nature will be widely feasible. Studying plant responses under refined lab conditions that more closely reflect natural conditions will likely fill the current gap between genetics and ecology and facilitate interdisciplinary communication between them in order to more holistically understand the underlying mechanisms of ever-changing phenological response in plants.

Methods:

Plant materials and growth conditions.

Except where indicated, all *Arabidopsis thaliana* plants, wild type (WT), *fkf1*(ref [17]), *fkf1–2* (ref [17]), *gi-2* (ref [22]), *ft-1* and *ft-1 tsf-1* (ref [64]), *ft-101* and *co-101* (ref [65]), *phyA-211* (ref [31]), *phyB-9* (ref [66]), *elf3–1* (ref [67]), *fhy1–3 fhl-1* (ref [33]), *cop1–6* (ref [68]), *spa1–3 spa3–1 spa4–1* (ref [69]), *pif1 pif3 pif4 pif5* (*pifq*)[70], *cry1* (*hy4–2.23N*) *cry2–1* (ref [71]), *cca1–1* lhy-Null* (ref [72]), *prr7–11 prr9–10* (ref [73]), *hos1–3* (ref [43]), *svp-32* and *svp-32 flm-3 flc-3* (ref [29]), *ELF3:ELF3–6H3F* and *ELF3:ELF3–6H3F/phyB-9* (ref [44]), *CO:HA-CO* and *35S:3HA-CO*[46], and *FT:GUS* [65], used in this study are in the Columbia-0 (Col-0) background. *phyA-201* is in the Landsberg *erecta* (L*er*) background[31]. The *ft-1* and *ft-1 tsf-1* seeds were kindly provided by Dr. Motomu Endo. The *fhy1–3 fhl-1* seeds were kindly provided by Dr. Mathias Zeidler. The *cop1–6* seeds were kindly provided by Dr. Xing Wang Deng. The *spa1–3 spa3–1 spa4–1* seeds were kindly provided by Dr. Ute Hoecker. The *cca1–1* lhy-Null* seeds were kindly provided by Drs. Rachel Green and Stacy Harmer. The *prr7–11 prr9–10* seeds were kindly provided by Dr. Takafumi Yamashino. The *svp-32* and *svp-32 flm-3 flc-3* seeds were kindly provided by Dr. Ji Hoon Ahn. Wild-type *Arabidopsis* accessions, Oy-1, RLD-1, Mh-0, An-1, Nos-0, Ma-1, Rd-0, Nd-1, En-1, Jl-3, Kz-9, Di-G, Wei-0, Ka-0, Sei-0, Mt-0, and Van-0 were all obtained from the ABRC stock center at Ohio State University. The *phyA-211 elf3–1* double mutant was generated by a genetic cross between *phyA-211* and *elf3–1*. The *co-101 elf3–1* double mutant was generated by a genetic cross between *co-101* and *elf3–1*.

To generate *35S:ELF3–6H3F* transgenic lines, the pENTR/D-TOPO vector harboring the full length of *ELF3* cDNA without a stop codon[44] was transferred to pB7HFC binary vector[44]. The *35S:ELF3–6H3F* construct in pB7HFC was transformed into *elf3–1* plants. For *ELF3:ELF3–6H3F/phyA-211* lines, the *ELF3:ELF3–6H3F* construct in pK7HFC vector[44] was introduced to *phyA-211* plants. To generate *35S:3HA-CO/35S:ELF3–6H3F* lines, the *35S:3HA-CO* construct in pH7WG2 (ref [46]) was transformed into the *35S:ELF3–6H3F* line. The transgenic plants were selected based on the expression levels of both *CO* and *ELF3* genes. For *CO:HA-CO/elf3–1* lines, the *CO:HA-CO* construct in pPZP221 binary vector[46] was transformed into *elf3–1* plants.

All plants were grown either on soil in standard flats with inserts (STF-1020-OPEN and STI-0804, T.O. Plastics; for plants grown in Seattle or similar flats/inserts for plants grown in Zürich and Edinburgh) or in sterile 1X Linsmaier and Skoog (LS) agar media (Caisson) without sucrose. The soil (Sunshine Mix #4, Sun Gro Horticulture) contained a slow release fertilizer (Osmocote 14–14-14, Scotts Miracle-Gro) and a pesticide (Systemic Granules,

Bonide). After seeds were sown onto soil or growth media, they were stratified in a 4°C room for at least three days and then transferred to outside growth areas or growth chambers. Only non-transgenic plants were used for the outdoor experiments, following institutional, national, and international restrictions on handing genetically modified organisms (transgenic plants were only used in certified lab settings). For outside experiments, the flats containing stratified seeds were transferred onto a platform in a low tunnel equipped with a shading filter in our caged plant growth areas (University of Washington, University of Zürich, and University of Edinburgh). To avoid shading effects from neighboring plants, seeds were sown at a low density, and when necessary, younger seedlings were thinned to let individuals grow separately. To prevent potential light stress from excess direct sunlight exposure (which can be stronger than 1000 μmol/m^2/s), the cage was covered with double layers of Reemay Garden Blanket (Reemay) to reduce sunlight intensity without changing the red/far-red ratio (R/FR). The R/FR ratio was measured by LightScout Red/Far Red meter (Spectrum Technologies), as well as UV-VIS Spectrometer (StellarNet Inc). The light intensity changes around the summer solstice were measured using LI-250A light meter (LI-COR). Temperature was directly monitored by HOBO Pendant Temperature/Light 64K Data Loggers (Onset) for Edinburgh as well as Seattle. Air temperature was obtained from nearby weather station data, https://www.ed.ac.uk/geosciences/weather-station/weather-station-data for Edinburgh, http://www.meteoswiss.admin.ch/home/research-and-cooperation/nccs.html for Zurich, and http://www-k12.atmos.washington.edu/k12/grayskies/nw_weather.html for Seattle, as shown in Supplementary Fig. 1. Information regarding sunrise time (ZT0) and day length in Seattle was obtained from http://aa.usno.navy.mil/data/docs/RS_OneYear.php.

Normal lab LD and SD conditions were described previously[46]. For FR light supplement in LD+FR and LD+FR+temp conditions, weak 730 nm far-red LED light (RAY “PfrSpec”, Fluence Bioengineering, previously referred to as BML Horticulture) was provided together with full-spectrum white fluorescent light (F017/950/24”, Octron Osram Sylvania) in order to set the R/FR=1. To obtain dim far-red light, we used a dimmer (Fluence Bioengineering/BML Horticulture) with the LED light source and also wrapped the LED light with a single layer of regular white copy paper. The R/FR ratio was adjusted using LightScout Red/Far Red meter (Spectrum Technologies), and confirmed using UV-VIS spectrometer.

To apply LD+light intensity conditions, light intensity changes during the daytime shown in Supplementary Fig. 8a were set based on averages of three day-long light intensity measurements shown in Fig. 1a. Specific settings in growth chambers were as follows: ZT0, 0 μmol/m^2/s; ZT1, 29 μmol/m^2/s; ZT4, 84 μmol/m^2/s; ZT7, 173 μmol/m^2/s; ZT10 148 μmol/m^2/s; ZT13, 81 μmol/m^2/s; and ZT16, 0 μmol/m^2/s. The light intensity between two settings was gradually changed in a ramping mode. The light intensity changes in the chamber were confirmed using LI-250A light sensor (LI-COR).

For temperature fluctuation settings in LD+temp and LD+FR+temp conditions, temperature data for seven days around the summer solstice of 2013, from June 21st to 27th, in Seattle was obtained from a website (http://www-k12.atmos.washington.edu/k12/grayskies/nw_weather.html) and averaged. Based on the average temperature data, a multi-step program shown in Supplementary Fig. 8g was set in ramping mode as follows: ZT0, 15.9°C;

ZT2, 16.2°C; ZT4, 17.9°C; ZT5.8, 19.4°C; ZT9, 22.2°C; ZT10.4, 22.6°C; ZT11, 22.8°C; ZT12, 22.1°C; ZT16, 19.8°C; ZT17, 18.3°C; ZT20, 16.6°C; ZT23, 15.8°C. The temperature changes were confirmed using HOBO Pendant Temperature/Light 64K Data Loggers (Onset).

Flowering time was measured by the number of rosette and cauline leaves on the main stem when inflorescence reached 1–5 cm high as described previously[46]. Flowering time experiments were performed with 12 individual plants at a minimum. All flowering time results in this manuscript are means ± standard errors of means (SEM).

RNA preparation and gene expression analyses.

For gene expression analyses, 14-day-old seedlings grown on soil (all outside grown samples) or LS agar plates (samples grown in the incubators) were harvested every 3 hours during a 24-h period and were used for RNA extraction. RNA extraction, cDNA synthesis, Q-PCR conditions and normalization by *IPP2*+*PP2A* were described previously[74]. Primers and PCR conditions for *CCA1*, *LHY*, *PRR9*, *PRR7*, *PRR5*, *TOC1*, *CDF1*, *FKF1*, *GI*, *CO*, *FT*, *FLC*, *SVP*, *ISOPENTENYL PYROPHOSPHATE/DIMETHYLALLYL PYROPHOSPHATE ISOMERASE* (*IPP2*), and *SERINE/THREONINE PROTEIN PHOSPHATASE 2A* (*PP2A*) were previously described[18, 19, 74, 75]. All expression results were normalized using averages of *IPP2* and *PP2A* values. The remaining primer sequences used for analyzing gene expression profiles are the following: `5′-GCACAGACTGATTAAGGTTCAAAAAC-3′` and `5′- CTTCACTGGATAGCTTTTAGCAG-3′` for `ELF3; 5′- AATCTAGAGATCAGGTTAACGC-3′` and `5′-CTTCTTCTGACACATCTTCCT-3′` for `PHYA; 5′-CTCGGGAATTCATCGTATTG-3′` and `5′-CCTCTGGCAGTTGAAGTAAG-3’` for *TSF*. Q-PCR for *CCA1*, *LHY*, *PRR9*, *PRR7*, *PRR5*, *TOC1*, *CDF1*, *GI*, *SVP*, and *IPP2* was done using the following program: 1 min at 95°C, followed by 40–50 cycles of 10 sec at 95°C and 20 sec at 60°C. Q-PCR for *FKF1*, *CO*, *FT*, *TSF*, *ELF3*, *PHYA*, and *PP2A* was done using the following program: 1 min at 95°C, followed by 40–50 cycles of 10 sec at 95°C, 15 sec at annealing temperature, and 15 sec at 72°C. Annealing temperature for each primer set was 55°C for *FKF1* and *CO*, 64°C for *FT*, 59°C for *TSF*, 61°C for *ELF3*, 64.3°C for *PHYA*, and 64°C for *PP2A.*

Whole transcriptome RNA-sequencing (RNA-seq) analysis.

Wild-type plants were grown on soil under LD, LD+FR+temp and natural LD conditions and harvested at ZT4 on day 14. The “2013 outside” samples were harvested on 6/25/13, and the “2014 outside” samples were harvested on 7/7/14. After mRNA was purified using NEB Next Poly(A) mRNA magnetic isolation kit (New England Biolabs), RNA-seq libraries were prepared using the YourSeq 3’-Digital Gene Expression RNAseq Library Kit (Amaryllis Nucleics). A Bioanalyzer 2100 (Agilent, High Sensitivity DNA Kit) was used for library quality control, to determine average library size, and together with concentration data from a Qubit 2.0 Fluorometer (Life Technologies, dsDNA High Sensitivity Assay Kit) to determine individual library molarity and pooled library molarity. Pooled libraries were sequenced on a NextSeq 500 (Illumina, High Output v2 75 cycle kit) to yield single-read 80 bp reads.

FASTQ sequence files were preprocessed in two steps. A Python library (clipper.py, https://github.com/mfcovington/clipper) was used to trim off the first 8 nucleotides of each read to remove potential mismatches to the reference sequence caused by annealing of a random hexamer required for library synthesis. Trimmomatic v0.36; http://www.usadellab.org/cms/?page=trimmomatic] was used to remove adapter sequences and trim or filter reads based on quality. The parameters used for Trimmomatic were “ILLUMINACLIP:TruSeq3-PE-2.fa: 2:30:10 LEADING:3 TRAILING:3 SLIDINGWINDOW:4:15 MINLEN:50”.

Preprocessed reads were mapped to the *Arabidopsis thaliana* TAIR10 cDNA reference sequence (ftp://ftp.ensemblgenomes.org/pub/plants/release-34/fasta/arabidopsis_thaliana/cdna/Arabidopsis_thaliana.TAIR10.cdna.all.fa.gz) using bowtie2 with the "--norc" parameter to enforce strand-specific alignment. Read counts for each transcript in the cDNA reference were calculated using a Perl script (simple_counts.pl, https://github.com/mfcovington/read_counter).

The R package edgeR[76] was used to identify differentially expressed transcripts between samples grown in lab LD conditions and samples grown in LD+FR+temp conditions, outdoor samples from 2013 and 2014. Transcripts were retained for analysis if they had more than two counts per million in at least three samples. After normalization factors were calculated and dispersion estimated, pairwise comparisons were performed using edgeR’s exact test. Differentially expressed genes were then filtered using a false discovery rate (FDR) cutoff of 0.05 and a minimum log2 fold change of 1. FDRs were calculated by adjusting P-values for multiple comparisons using the Benjamini–Hochberg procedure[77].

Differential gene expression results were annotated using TAIR10 gene and transcript descriptions (https://www.arabidopsis.org/download_files/Genes/TAIR10_genome_release/gene_description_20131231.txt.gz). Gene ontology analysis was performed using DAVID[78].

GUS staining.

For histochemical staining of GUS activity for tissue-specific expression of the *FT* gene, 14-day-old *FT:GUS* plants grown under LD, LD+FR and LD+FR+temp conditions were harvested either at ZT4 (LD+FR and LD+FR+temp grown samples) or at both ZT4 and ZT16 (LD grown samples), and immediately treated with 90% pre-chilled acetone on ice for 10–15 min to fix and extract chlorophylls. After washing three times with 100 mM Na-phosphate pH7.0, whole plant tissues were submerged in the staining solution (100 mM Na-phosphate pH7.0, 10 mM EDTA, 0.5 mM Potassium ferricyanide, 0.5 mM Potassium ferrocyanide, 0.1% Triton X-100, and 1 mM X-Gluc). After 4-hour staining, the tissues were washed and dehydrated with ethanol series 30%, 50%, 80%, and 100%.

Tandem affinity purification coupled mass spectrometry (TAP-MS) analysis.

Fourteen-day-old *ELF3:ELF3–6H3F, ELF3:ELF3–6H3F/phyA-211* and *ELF3:ELF3–6H3F/phyB-9* lines grown on LS agar plates under the LD+FR+temp conditions were harvested at ZT4. Procedures for Tandem FLAG and His-immunoprecipitations (IP), protein digestion, and liquid chromatography-tandem mass spectrometry (LC-MS/MS) were performed according to Huang *et al.*[44].

Statistical analysis.

Statistical analyses for flowering time experiments were done using R Statistical Computing software (v3.2.3; R Core Team, 2015). The effect of conditions on flowering time was tested using linear models (lm) when the assumptions were met in 'gvlma' function in the 'gvlma' package. When the assumptions were not met, generalized linear models (glm) with poisson error distribution (faily=poisson) were used. For more than two groups, pairwise comparisons were conducted with Tukey's multiple comparisons adjustment using 'glht' function in the 'multcomp' package.

Immunoblot analysis and protein quantification.

For analyzing diurnal expression profiles of phyA, ELF3, and CO proteins, 14-day-old *Arabidopsis* seedlings grown on LS agar media under LD or LD+FR+temp conditions were harvested at each time point, frozen in liquid nitrogen, and stored at −80 ºC. Total proteins were extracted using extraction buffer [50 mM Na-phosphate pH7.4, 100 mM NaCl, 10% glycerol, 5 mM EDTA, 1 mM DTT, 1% NP-40, 0.5% SDS, 0.5% Sodium deoxycholate, 50 μM MG-132, 2 mM $NaVO_4$, 2 mM NaF, and protease inhibitor tablets-EDTA free (Pierce)], and nuclei samples were prepared using CelLytic Plant Nuclei Isolation/Extraction Kit (Sigma) based on manufacturer protocol.

To detect proteins, total protein extract for phyA and ELF3, or nuclear extract for CO, were resolved in 9% or 11–12% SDS-PAGE gels, respectively, and transferred to nitrocellulose membranes (Bio-rad). phyA, ELF3–6H3F, and HA-CO proteins were detected using a monoclonal anti-phyA antibody[79] kindly provided by Dr. Akira Nagatani, anti-FLAG (A8592, Sigma), and anti-HA (3F10, Roche) antibodies. Actin or Histone H3 proteins were used for internal loading controls of total protein or nuclear extract, respectively, and detected by anti-actin (C4, Millipore) and anti-histone H3 (ab1791, Abcam) antibodies, respectively.

For protein quantification, immunoreactive proteins on immunoblotted membranes were visualized with SuperSignal West Pico Luminol/Enhanced Solution (Thermo) and/or ECL Select Western Blotting Detection Reagent (Amersham) and imaged by ChemiDoc Touch (Bio-rad). The image was used for quantification with the Image Lab program (Bio-rad). Relative protein abundance was normalized against Actin or Histone H3.

Co-immunoprecipitation experiments.

To analyze *in vivo* interactions, the *ELF3:ELF3–6H3F*, *35S:ELF3–6H3F*[44], *35S:3HA-CO*, and *35S:3HA-CO 35S:ELF3–6H3F* lines grown under LD, LD+FR, or LD+FR+temp conditions were harvested at ZT0, ZT2, or ZT4 on day 14, frozen in liquid nitrogen, and stored at −80 ºC. For analyzing *in planta* interactions, the *35S:ELF3–6H3F*, *35S:3HA-CO*[46], and *35S:CO-TAP*[46] constructs were infiltrated into 3-week-old *Nicotiana benthamiana* leaves as described[46].

The method for coimmunoprecipitation (Co-IP) assays was described previously[46]. Briefly, proteins were extracted from 1 ml volume of ground tissues using Co-IP buffer [50 mM Na-phosphate pH7.4, 150 mM NaCl, 10% glycerol, 5 mM EDTA, 1 mM DTT, 0.1% Triton

X-100, 50 μM MG-132, 2 mM $NaVO_4$, 2 mM NaF, and protease inhibitor tablets-EDTA free (Pierce)] and incubated with Protein G-coupled magnetic beads (Dynabeads Protein G, Invitrogen) that captured anti-FLAG (F1804, Sigma) antibody at 4 ºC for 10 minutes under dim light. After washing three times, precipitated proteins were eluted with 2X SDS sample buffer at 80 ºC for three minutes. Fifty percent of the eluted proteins and 1.5% of the total extract as an input were resolved in 9% SDS-PAGE gels. ELF-6H3F and endogenous phyA proteins were detected by western blot using anti-FLAG (Sigma) and anti-phyA antibodies, respectively.

Supplementary Material

Refer to Web version on PubMed Central for supplementary material.

Acknowledgments:

We thank Drs. Motomu Endo, Mathias Zeidler, Xing Wang Deng, Ute Hoecker, Rachel Green, Stacey Harmer, Takafumi Yamashino, and Ji Hoon Ahn for providing the mutant seeds, Dr. Jennifer Nemhauser for critical reading of the manuscript, and Jeanette Milne for technical support. This work was supported by NIH grant (GM079712) to T.I., NSF grants (IOS-1656076 to TI, and IOS-1456796 to D.A.N.), Next-Generation BioGreen 21 Program (SSAC, PJ013386, Rural Development Administration, Republic of Korea) to Y.H.S. and T.I., JST CREST Grant (JPMJCR16O3), MEXT Kakenhi (18H04785) and Swiss National Science Foundation to K.K.S., and NRF grant (NRF-2015R1D1A1A01058948) to Y.H.S. We acknowledge NSF grant (DBI-0922879) for LTQ-Velos Pro Orbitrap LC-MS/MS acquisition. A.K. is supported by the JSPS Postdoctoral Fellowships for Research Abroad.

References:

1. Song YH, Shim JS, Kinmonth-Schultz HA, Imaizumi T. Photoperiodic flowering: time measurement mechanisms in leaves. Annu. Rev. Plant Biol. 66, 441–464 (2015). [PubMed: 25534513]
2. Mouradov A, Cremer F, Coupland G. Control of flowering time: interacting pathways as a basis for diversity. Plant Cell 14 Suppl., S111–130 (2002).
3. Song YH, Ito S, Imaizumi T. Flowering time regulation: photoperiod- and temperature-sensing in leaves. Trends Plant Sci. 18, 575–583 (2013). [PubMed: 23790253]
4. Golembeski GS, Imaizumi T. Photoperiodic regulation of florigen function in Arabidopsis thaliana. Arabidopsis Book 13, e0178 (2015). [PubMed: 26157354]
5. Blümel M, Dally N, Jung C. Flowering time regulation in crops-what did we learn from Arabidopsis? Curr. Opin. Biotechnol. 32, 121–129 (2015). [PubMed: 25553537]
6. Kubota A, Kita S, Ishizaki K, Nishihama R, Yamato KT, Kohchi T. Co-option of a photoperiodic growth-phase transition system during land plant evolution. Nat. Commun. 5, 3668 (2014). [PubMed: 24752248]
7. Mockler T, et al. Regulation of photoperiodic flowering by Arabidopsis photoreceptors. Proc. Natl. Acad. Sci. USA 100, 2140–2145 (2003). [PubMed: 12578985]
8. Ratcliffe D The geographical and ecological distribution of Arabidopsis and comments on physiological variation. Arabidopsis Information Service 1 Suppl, (1965).
9. Effmertova E The behaviour of “summer annual”, “mixed”, and “winter annual” natural populations as compared with early and late races in field conditions. Arabidopsis Information Service 4, (1967).
10. Thompson L The spatiotemporal effects of nitrogen and litter on the population dynamics of Arabidopsis thaliana. J. Ecol. 82, 63–68 (1994).
11. Donohue K Germination timing influences natural selection on life-history characters in Arabidopsis thaliana. Ecology 83, 1006–1016 (2002).

12. Griffith C, Kim E, Donohue K. Life-history variation and adaptation in the historically mobile plant Arabidopsis thaliana (Brassicaceae) in North America. Am. J. Bot. 91, 837–849 (2004). [PubMed: 21653439]
13. Wilczek AM, et al. Effects of genetic perturbation on seasonal life history plasticity. Science 323, 930–934 (2009). [PubMed: 19150810]
14. Picó FX. Demographic fate of Arabidopsis thaliana cohorts of autumn- and spring-germinated plants along an altitudinal gradient. J. Ecol. 100, 1009–1018 (2012).
15. Chiang GCK, Barua D, Dittmar E, Kramer EM, de Casas RR, Donohue K. Pleiotropy in the wild: the dormancy gene DOG1 exerts cascading control on life cycles. Evolution 67, 883–893 (2013). [PubMed: 23461337]
16. Bieniawska Z, Espinoza C, Schlereth A, Sulpice R, Hincha DK, Hannah MA. Disruption of the Arabidopsis circadian clock is responsible for extensive variation in the cold-responsive transcriptome. Plant Physiol. 147, 263–279 (2008). [PubMed: 18375597]
17. Imaizumi T, Tran HG, Swartz TE, Briggs WR, Kay SA. FKF1 is essential for photoperiodic-specific light signalling in Arabidopsis. Nature 426, 302–306 (2003). [PubMed: 14628054]
18. Imaizumi T, Schultz TF, Harmon FG, Ho LA, Kay SA. FKF1 F-box protein mediates cyclic degradation of a repressor of CONSTANS in Arabidopsis. Science 309, 293–297 (2005). [PubMed: 16002617]
19. Kinmonth-Schultz HA, et al. Cool night-time temperatures induce the expression of CONSTANS and FLOWERING LOCUS T to regulate flowering in Arabidopsis. New Phytol. 211, 208–224 (2016). [PubMed: 26856528]
20. Yamaguchi A, Kobayashi Y, Goto K, Abe M, Araki T. TWIN SISTER OF FT (TSF) acts as a floral pathway integrator redundantly with FT. Plant Cell Physiol. 46, 1175–1189 (2005). [PubMed: 15951566]
21. Krzymuski M, et al. The dynamics of FLOWERING LOCUS T expression encodes long-day information. Plant J. 83, 952–961 (2015). [PubMed: 26212862]
22. Mizoguchi T, et al. Distinct roles of GIGANTEA in promoting flowering and regulating circadian rhythms in Arabidopsis. Plant Cell 17, 2255–2270 (2005). [PubMed: 16006578]
23. <au>Amasino R. Seasonal and developmental timing of flowering. Plant J. 61, 1001–1013 (2010). [PubMed: 20409274]
24. Holmes MG, Smith H. The function of phytochrome in plants growing in the natural environment. Nature 254, 512–514 (1975).
25. Wollenberg AC, Strasser B, Cerdan PD, Amasino RM. Acceleration of flowering during shade avoidance in Arabidopsis alters the balance between FLOWERING LOCUS C-mediated repression and photoperiodic induction of flowering. Plant Physiol. 148, 1681–1694 (2008). [PubMed: 18790998]
26. Kim SY, Yu X, Michaels SD. Regulation of CONSTANS and FLOWERING LOCUS T expression in response to changing light quality. Plant Physiol. 148, 269–279 (2008). [PubMed: 18667727]
27. Bouché F, Lobet G, Tocquin P, Périlleux C. FLOR-ID: an interactive database of flowering-time gene networks in Arabidopsis thaliana. Nucleic. Acids Res. 44, D1167–1171 (2016). [PubMed: 26476447]
28. Koornneef M, Alonso-Blanco C, Vreugdenhil D. Naturally occurring genetic variation in Arabidopsis thaliana. Annu. Rev. Plant Biol. 55, 141–172 (2004). [PubMed: 15377217]
29. Lee JH, et al. Regulation of temperature-responsive flowering by MADS-box transcription factor repressors. Science 342, 628–632 (2013). [PubMed: 24030492]
30. Pruneda-Paz JL, Kay SA. An expanding universe of circadian networks in higher plants. Trends Plant Sci. 15, 259–265 (2010). [PubMed: 20382065]
31. Reed JW, Nagatani A, Elich TD, Fagan M, Chory J. Phytochrome A and phytochrome B have overlapping but distinct functions in Arabidopsis development. Plant Physiol. 104, 1139–1149 (1994). [PubMed: 12232154]
32. Johnson E, Bradley M, Harberd NP, Whitelam GC. Photoresponses of light-grown phyA mutants of Arabidopsis (Phytochrome A is required for the perception of daylength extensions). Plant Physiol. 105, 141–149 (1994). [PubMed: 12232194]

33. Genoud T, et al. FHY1 mediates nuclear import of the light-activated phytochrome A photoreceptor. PLoS Genet. 4, e1000143 (2008). [PubMed: 18670649]
34. Mockler TC, Guo H, Yang H, Duong H, Lin C. Antagonistic actions of Arabidopsis cryptochromes and phytochrome B in the regulation of floral induction. Development 126, 2073–2082 (1999). [PubMed: 10207133]
35. Valverde F, Mouradov A, Soppe W, Ravenscroft D, Samach A, Coupland G. Photoreceptor regulation of CONSTANS protein in photoperiodic flowering. Science 303, 1003–1006 (2004). [PubMed: 14963328]
36. Reed JW, et al. Independent action of ELF3 and phyB to control hypocotyl elongation and flowering time. Plant Physiol. 122, 1149–1160 (2000). [PubMed: 10759510]
37. Leivar P, Quail PH. PIFs: pivotal components in a cellular signaling hub. Trends Plant Sci. 16, 19–28 (2011). [PubMed: 20833098]
38. Nusinow DA, et al. The ELF4-ELF3-LUX complex links the circadian clock to diurnal control of hypocotyl growth. Nature 475, 398–402 (2011). [PubMed: 21753751]
39. Jang S, et al. Arabidopsis COP1 shapes the temporal pattern of CO accumulation conferring a photoperiodic flowering response. EMBO J. 27, 1277–1288 (2008). [PubMed: 18388858]
40. Laubinger S, et al. Arabidopsis SPA proteins regulate photoperiodic flowering and interact with the floral inducer CONSTANS to regulate its stability. Development 133, 3213–3222 (2006). [PubMed: 16854975]
41. Nakamichi N, et al. Arabidopsis clock-associated pseudo-response regulators PRR9, PRR7 and PRR5 coordinately and positively regulate flowering time through the canonical CONSTANS-dependent photoperiodic pathway. Plant Cell Physiol. 48, 822–832 (2007). [PubMed: 17504813]
42. Park MJ, Kwon YJ, Gil KE, Park CM. LATE ELONGATED HYPOCOTYL regulates photoperiodic flowering via the circadian clock in Arabidopsis. BMC Plant Biol. 16, 114 (2016). [PubMed: 27207270]
43. Lazaro A, Valverde F, Pineiro M, Jarillo JA. The Arabidopsis E3 ubiquitin ligase HOS1 negatively regulates CONSTANS abundance in the photoperiodic control of flowering. Plant Cell 24, 982–999 (2012). [PubMed: 22408073]
44. Huang H, et al. Identification of evening complex associated proteins in Arabidopsis by affinity purification and mass spectrometry. Mol. Cell Proteomics 15, 201–217 (2016). [PubMed: 26545401]
45. Schwartz CJ, Lee J, Amasino R. Variation in shade-induced flowering in Arabidopsis thaliana results from FLOWERING LOCUS T allelic variation. PLoS One 12, e0187768 (2017). [PubMed: 29117199]
46. Song YH, Smith RW, To BJ, Millar AJ, Imaizumi T. FKF1 conveys timing information for CONSTANS stabilization in photoperiodic flowering. Science 336, 1045–1049 (2012). [PubMed: 22628657]
47. Yu JW, et al. COP1 and ELF3 control circadian function and photoperiodic flowering by regulating GI stability. Mol. Cell 32, 617–630 (2008). [PubMed: 19061637]
48. Sheerin DJ, et al. Light-activated phytochrome A and B interact with members of the SPA family to promote photomorphogenesis in Arabidopsis by reorganizing the COP1/SPA complex. Plant Cell 27, 189–201 (2015). [PubMed: 25627066]
49. Kim WY, Hicks KA, Somers DE. Independent roles for EARLY FLOWERING 3 and ZEITLUPE in the control of circadian timing, hypocotyl length, and flowering time. Plant Physiol. 139, 1557–1569 (2005). [PubMed: 16258016]
50. Lin MK, et al. FLOWERING LOCUS T protein may act as the long-distance florigenic signal in the cucurbits. Plant Cell 19, 1488–1506 (2007). [PubMed: 17540715]
51. Yoo SC, et al. Phloem long-distance delivery of FLOWERING LOCUS T (FT) to the apex. Plant J. 75, 456–468 (2013). [PubMed: 23607279]
52. Mitchell DE, Gadus MV, Madore MA. Patterns of assimilate production and translocation in muskmelon (Cucumis melo L.) : I. diurnal patterns. Plant Physiol. 99, 959–965 (1992). [PubMed: 16669025]

53. Savage JA, Zwieniecki MA, Holbrook NM. Phloem transport velocity varies over time and among vascular bundles during early cucumber seedling development. Plant Physiol. 163, 1409–1418 (2013). [PubMed: 24072581]
54. Yasunaga E, Yano T, Araki T, Setoyama S, Kitano M. Effect of environmental condition on xylem and phloem transport of developing fruit. IFAC Proc. Vol 46, 297–301 (2013).
55. Shim JS, Kubota A, Imaizumi T. Circadian clock and photoperiodic flowering in Arabidopsis: CONSTANS Is a hub for signal integration. Plant Physiol. 173, 5–15 (2017). [PubMed: 27688622]
56. Pittendrigh CS, Minis DH. The entrainment of circadian oscillations by light and their role as photoperiodic clocks. Am. Nat. 98, 261–294 (1964).
57. Gattermann R, et al. Golden hamsters are nocturnal in captivity but diurnal in nature. Biol. Lett. 4, 253–255 (2008). [PubMed: 18397863]
58. Daan S, et al. Lab mice in the field: unorthodox daily activity and effects of a dysfunctional circadian clock allele. J. Biol. Rhythms 26, 118–129 (2011). [PubMed: 21454292]
59. Vanin S, et al. Unexpected features of Drosophila circadian behavioural rhythms under natural conditions. Nature 484, 371–375 (2012). [PubMed: 22495312]
60. Montelli S, et al. period and timeless mRNA splicing profiles under natural conditions in Drosophila melanogaster. J. Biol. Rhythms 30, 217–227 (2015). [PubMed: 25994101]
61. Shimizu KK, Kudoh H, Kobayashi MJ. Plant sexual reproduction during climate change: gene function in natura studied by ecological and evolutionary systems biology. Ann. Bot. 108, 777–787 (2011). [PubMed: 21852275]
62. Kudoh H Molecular phenology in plants: in natura systems biology for the comprehensive understanding of seasonal responses under natural environments. New Phytol. 210, 399–412 (2016). [PubMed: 26523957]
63. Jefferson RA, Kavanagh TA, Bevan MW. GUS fusions: beta-glucuronidase as a sensitive and versatile gene fusion marker in higher plants. EMBO J. 6, 3901–3907 (1987). [PubMed: 3327686]
64. Kotake T, Takada S, Nakahigashi K, Ohto M, Goto K. Arabidopsis TERMINAL FLOWER 2 gene encodes a heterochromatin protein 1 homolog and represses both FLOWERING LOCUS T to regulate flowering time and several floral homeotic genes. Plant Cell Physiol. 44, 555–564 (2003). [PubMed: 12826620]
65. Takada S, Goto K. TERMINAL FLOWER2, an Arabidopsis homolog of HETEROCHROMATIN PROTEIN1, counteracts the activation of FLOWERING LOCUS T by constans in the vascular tissues of leaves to regulate flowering time. Plant Cell 15, 2856–2865 (2003). [PubMed: 14630968]
66. Reed JW, Nagpal P, Poole DS, Furuya M, Chory J. Mutations in the gene for the red/far-red light receptor phytochrome B alter cell elongation and physiological responses throughout Arabidopsis development. Plant Cell 5, 147–157 (1993). [PubMed: 8453299]
67. Liu XL, Covington MF, Fankhauser C, Chory J, Wagner DR. ELF3 encodes a circadian clock-regulated nuclear protein that functions in an Arabidopsis PHYB signal transduction pathway. Plant Cell 13, 1293–1304 (2001). [PubMed: 11402161]
68. McNellis TW, von Arnim AG, Araki T, Komeda Y, Misera S, Deng XW. Genetic and molecular analysis of an allelic series of cop1 mutants suggests functional roles for the multiple protein domains. Plant Cell 6, 487–500 (1994). [PubMed: 8205001]
69. Laubinger S, Fittinghoff K, Hoecker U. The SPA quartet: a family of WD-repeat proteins with a central role in suppression of photomorphogenesis in Arabidopsis. Plant Cell 16, 2293–2306 (2004). [PubMed: 15308756]
70. Leivar P, et al. Multiple phytochrome-interacting bHLH transcription factors repress premature seedling photomorphogenesis in darkness. Curr. Biol. 18, 1815–1823 (2008). [PubMed: 19062289]
71. Yanovsky MJ, Mazzella MA, Whitelam GC, Casal JJ. Resetting of the circadian clock by phytochromes and cryptochromes in Arabidopsis. J. Biol. Rhythms 16, 523–530 (2001). [PubMed: 11760010]
72. Yakir E, Hilman D, Kron I, Hassidim M, Melamed-Book N, Green RM. Posttranslational regulation of CIRCADIAN CLOCK ASSOCIATED1 in the circadian oscillator of Arabidopsis. Plant Physiol. 150, 844–857 (2009). [PubMed: 19339503]

73. Nakamichi N, Kita M, Ito S, Yamashino T, Mizuno T. PSEUDO-RESPONSE REGULATORS, PRR9, PRR7 and PRR5, together play essential roles close to the circadian clock of Arabidopsis thaliana. Plant Cell Physiol. 46, 686–698 (2005). [PubMed: 15767265]

74. Kubota A, et al. TCP4-dependent induction of CONSTANS transcription requires GIGANTEA in photoperiodic flowering in Arabidopsis. PLoS Genet. 13, e1006856 (2017). [PubMed: 28628608]

75. Baudry A, et al. F-box proteins FKF1 and LKP2 act in concert with ZEITLUPE to control Arabidopsis clock progression. Plant Cell 22, 606–622 (2010). [PubMed: 20354196]

76. Robinson MD, McCarthy DJ, Smyth GK. edgeR: a Bioconductor package for differential expression analysis of digital gene expression data. Bioinformatics 26, 139–140 (2010). [PubMed: 19910308]

77. Benjamini Y, Hochberg Y. Controlling the false discovery rate: a practical and powerful approach to multiple testing. J. R. Stat. Soc. Series B Stat. Methodol. 57, 289–300 (1995).

78. Huang da W, Sherman BT, Lempicki RA. Systematic and integrative analysis of large gene lists using DAVID bioinformatics resources. Nat. Protoc. 4, 44–57 (2009). [PubMed: 19131956]

79. Shinomura T, Nagatani A, Hanzawa H, Kubota M, Watanabe M, Furuya M. Action spectra for phytochrome A- and B-specific photoinduction of seed germination in Arabidopsis thaliana. Proc. Natl. Acad. Sci. USA 93, 8129–8133 (1996). [PubMed: 8755615]

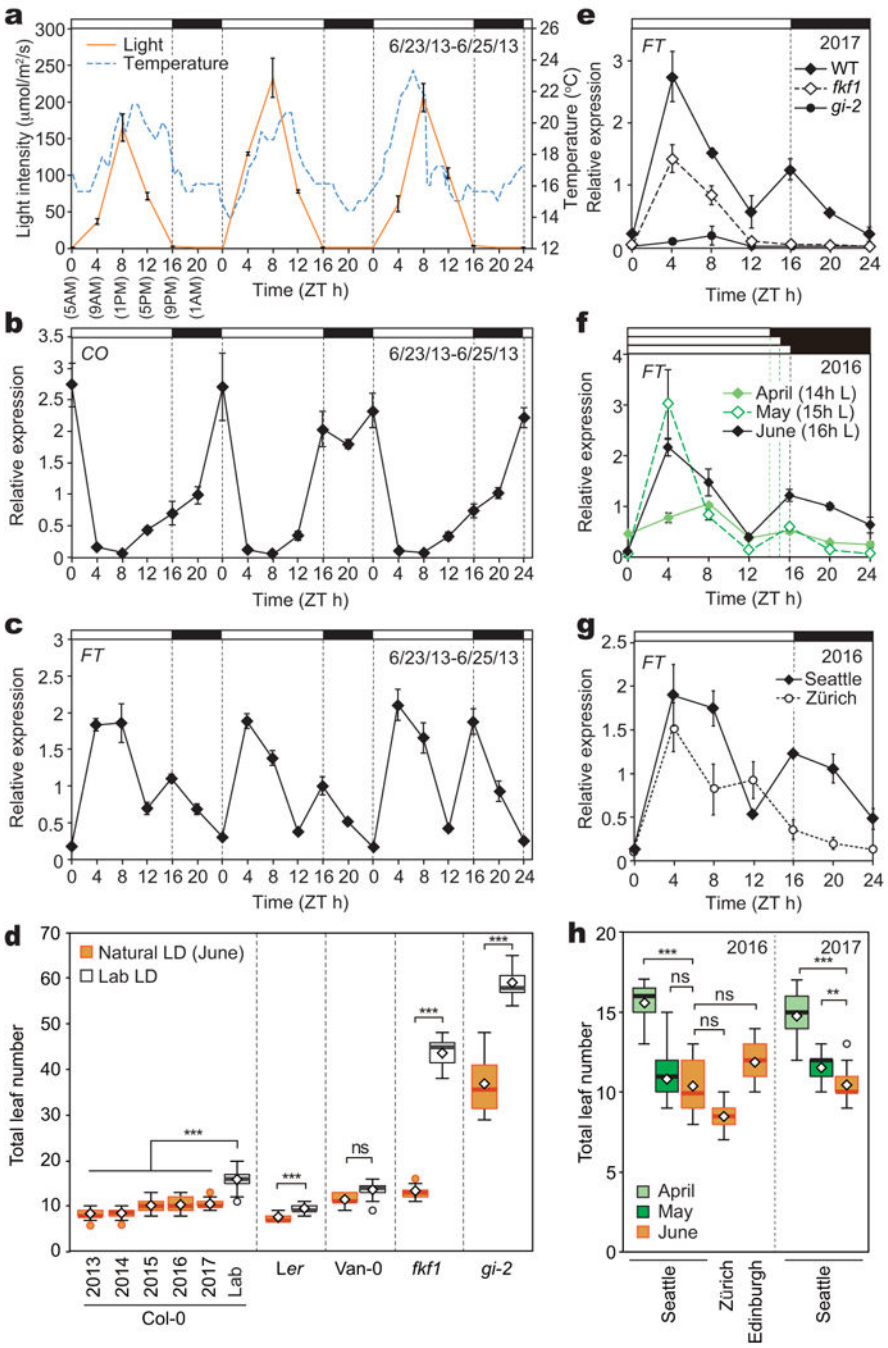

Fig. 1: The florigen FT gene is induced in the morning in natural LD.

a, Changes in light intensity and temperature on the days near the summer solstice in 2013 when the samples were harvested. For outside conditions, Zeitgeber time 0 (ZT0) was set as the sunrise time (i.e. 5 AM in Seattle from 6/23/13 to 6/25/13). Light intensity results are means ± SEM from different growth areas (n=3). Temperature data were obtained from a nearby weather station. **b**, **c**, Expression profiles of *CO* (**b**) and *FT* (**c**) under the conditions shown in (**a**). All gene expression results (means ± SEM) in this manuscript were normalized against *IPP2* and *PP2A* (n=3 biologically independent samples). **d**, Flowering

time results of plants grown outside in June and in lab LD. Each box is located between the upper and the lower quartiles, and the whiskers indicate 1.5-times interquartile ranges. The thick horizontal lines in the boxes represent the median, and open diamonds represent the mean. Outliers are indicated by circles. ($12 \leq n \leq 100$, *** $p<0.001$, ns: non-significant, linear models or generalized linear models were used throughout the manuscript. See detail statistical information in Supplementary Table 3). **e**, *FT* expression profiles in wild-type (WT: Col-0) plants, *fkf1*, and *gi-2* mutants grown outside around the summer solstice. **f**, *FT* expression profiles in WT grown at different times in spring. **g**, *FT* expression profiles in WT grown around the summer solstice in Seattle and Zürich. (for **e**-**g**, n=3 biologically independent samples). **h**, Flowering phenotypes of WT plants grown in different months and locations in spring. The details of the box plots are the same as those in Fig. 1d ($n \geq 11$, ** $p<0.01$, *** $p<0.001$, ns: non-significant, statistical information in Supplementary Table 3).

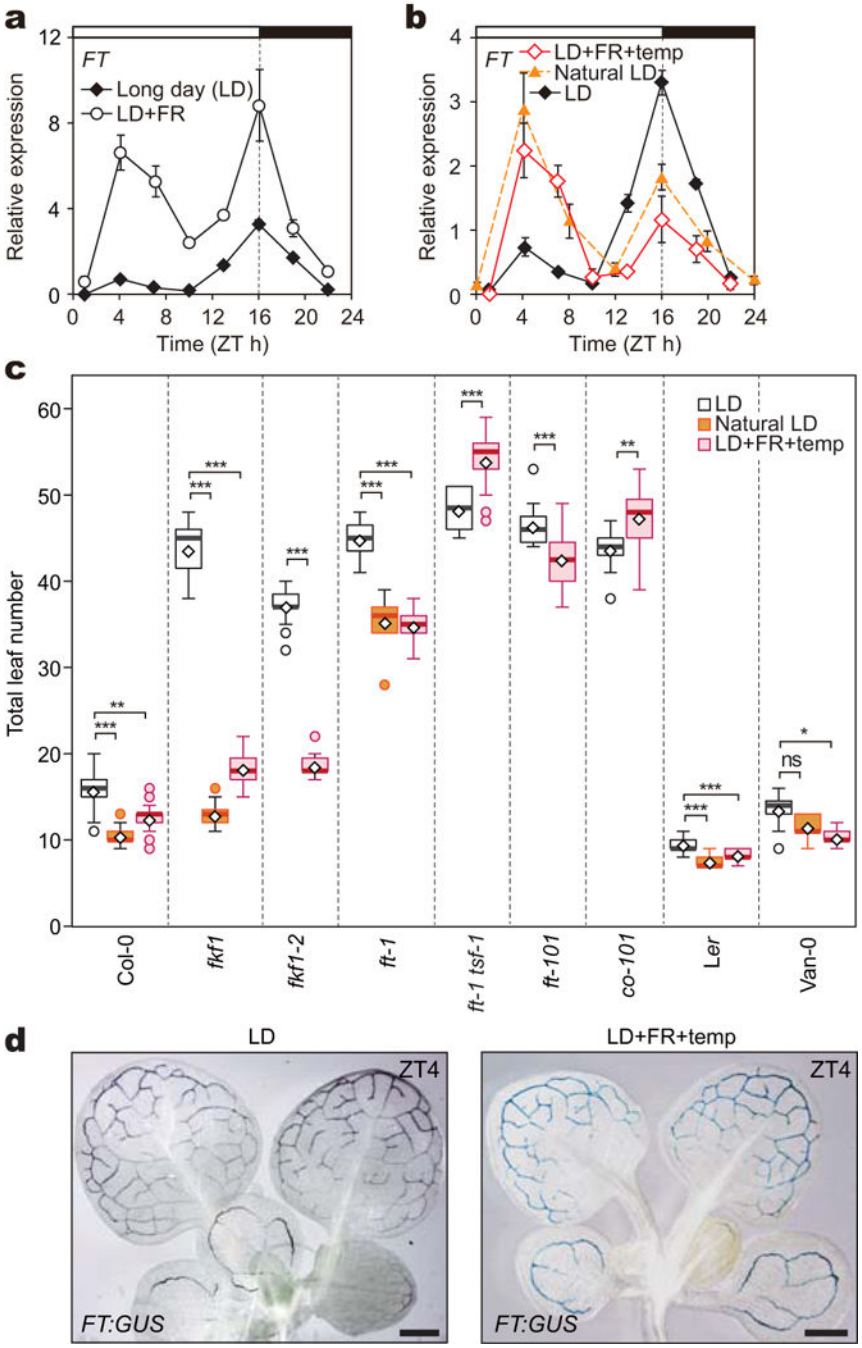

Fig. 2: Adjusting the R/FR ratio to 1 and changing the daily temperature of the lab growth conditions are sufficient to recreate the FT profiles and flowering of plants grown in natural LD.

a, **b,** *FT* expression profiles in LD and LD+FR (**a**), and in LD, LD+FR+temp, and outside in 2014 (**b**). The results represent means ± SEM (n=3 biologically independent samples). **c**, Flowering phenotypes of WT accessions and photoperiodic mutants in LD+FR+temp. Each box is located between the upper and the lower quartiles, and the whiskers indicate 1.5-times interquartile ranges. The thick horizontal lines in the boxes represent the median, and open diamonds represent the mean. Outliers are indicated by circles. (n≥11, * p<0.05, ** p<0.01,

*** $p<0.001$, ns: non-significant, statistical information in Supplementary Table 3). **d**, Spatial expression patterns of *FT* in LD+FR+temp. *FT:GUS* plants were grown in LD+FR +temp for two weeks and harvested at ZT4 (n=4–5 independent plants, repeated twice biologically). As a comparison, the *FT:GUS* plants were grown in LD and harvested at ZT4 (n=5 independent plants). The staining patterns of GUS activity in the LD-grown samples harvested in ZT4 resembled those in the ones harvested at the end of the day (ZT16) (Supplementary Fig. 13), most likely due to the very stable nature of the GUS protein[63]. Scale bar=1 mm.

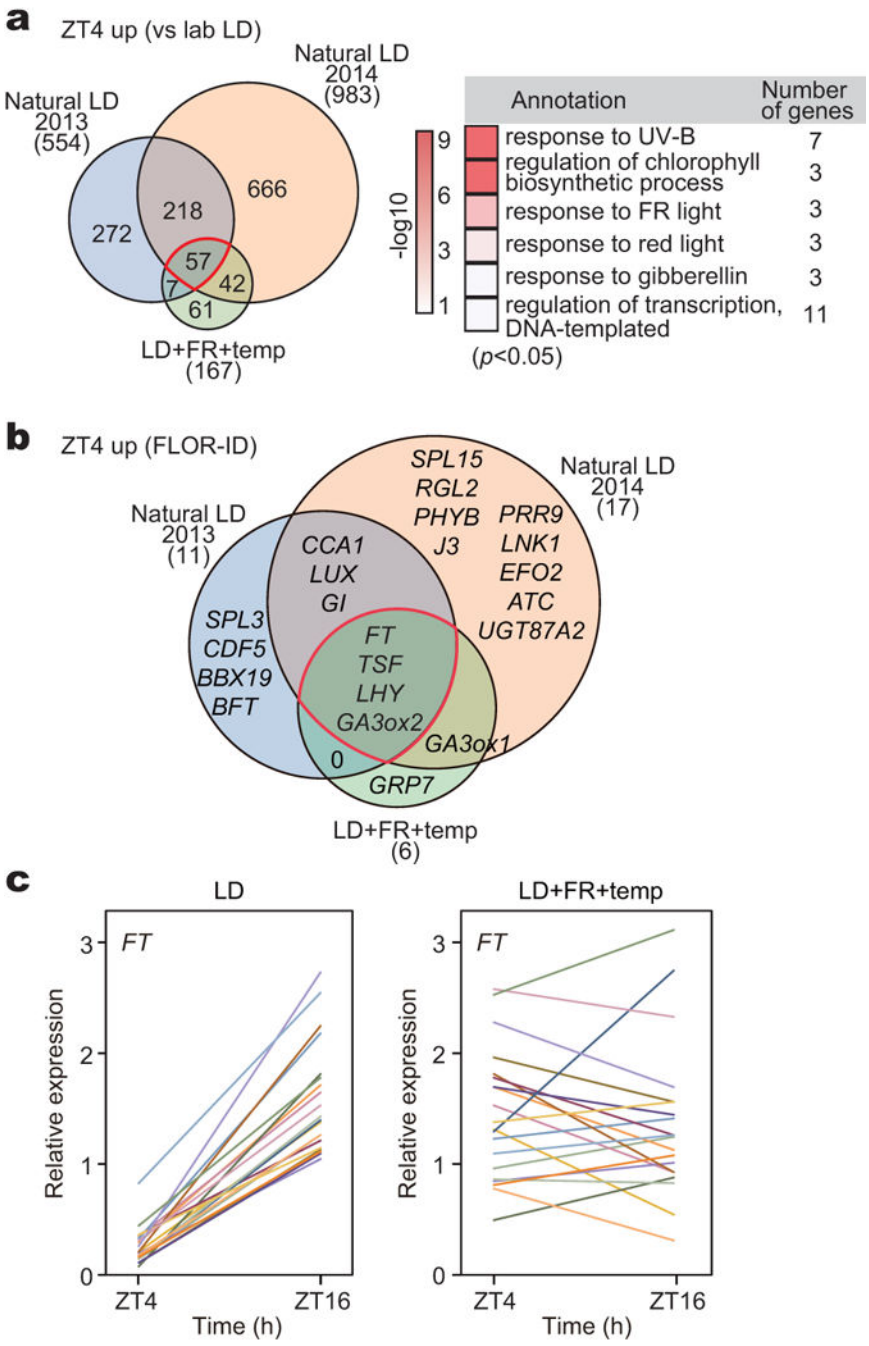

Fig. 3: Morning induction of florigen expression occurs under both natural LD and LD+FR +temp conditions, and is a common response in wild-type accessions.

a, The upregulated genes of RNA-seq results in two-week-old samples harvested at ZT4 in 2013, 2014, and LD+FR+temp conditions compared with the ZT4 samples in LD (n=3 biologically independent samples). The GO term categories enriched in the 57 genes are shown. The *p*-values represent one-tail Fisher Exact Probability Values. See Supplementary Table 1 for the actual values. **b**, Flowering-related genes in FLOR-ID were extracted from

the dataset shown in (E). **c**, *FT* expression levels in the morning (ZT4) and at dusk (ZT16) in 20 *Arabidopsis* WT accessions (Supplementary Fig. 15) in LD and LD+FR+temp.

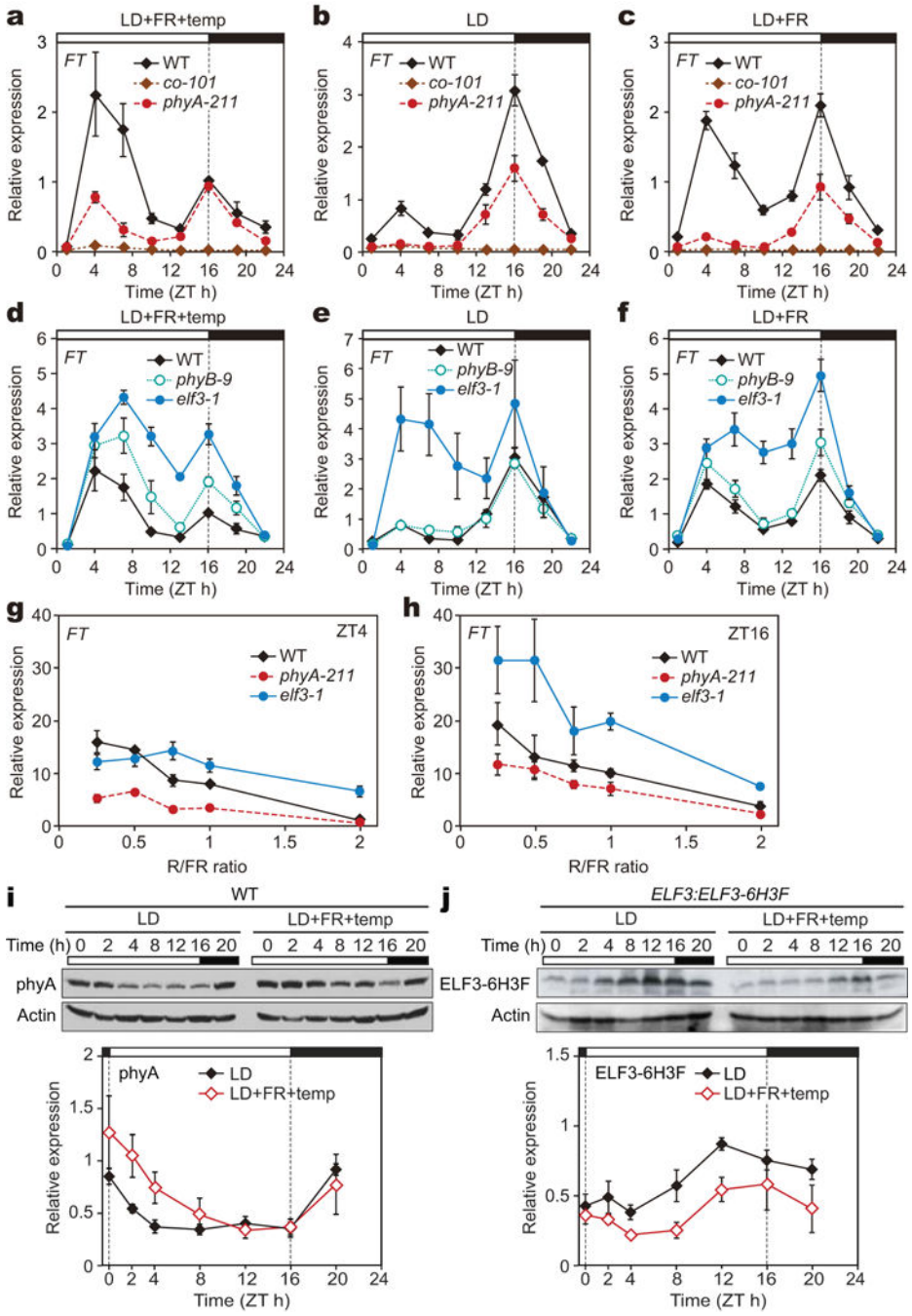

Fig. 4: phyA and ELF3 are involved in the regulation of morning FT expression in LD+FR +temp.

a-c, *FT* expression profiles in WT plants, *co-101*, and *phyA-211* mutants in LD+FR+temp (**a**), LD (**b**), and LD+FR (**c**). **d-f**, *FT* expression profiles in WT plants, *phyB-9*, and *elf3–1* mutants in LD+FR+temp (**d**), LD (**e**), and LD+FR (**f**). **g**, **h**, *FT* levels in WT plants, *phyA-211*, and *elf3–1* mutants in LD with different R/FR ratios. The levels of *FT* in these plants in the morning, ZT4 (**g**), and at dusk, ZT16 (**h**). For **a-h**, the results represent means ± SEM (n=3 biologically independent samples). **i**, Daily accumulation patterns of phyA

protein in LD and LD+FR+temp. **j**, Daily accumulation patterns of ELF3 protein in *ELF3:ELF3–6H3F* plants in LD and LD+FR+temp. For both (**i**) and (**j**), the representative blot images are shown. Actin was used as a loading control. The protein quantification results (relative values against the loading control) represent means ± SEM (n=6 biologically independent samples).

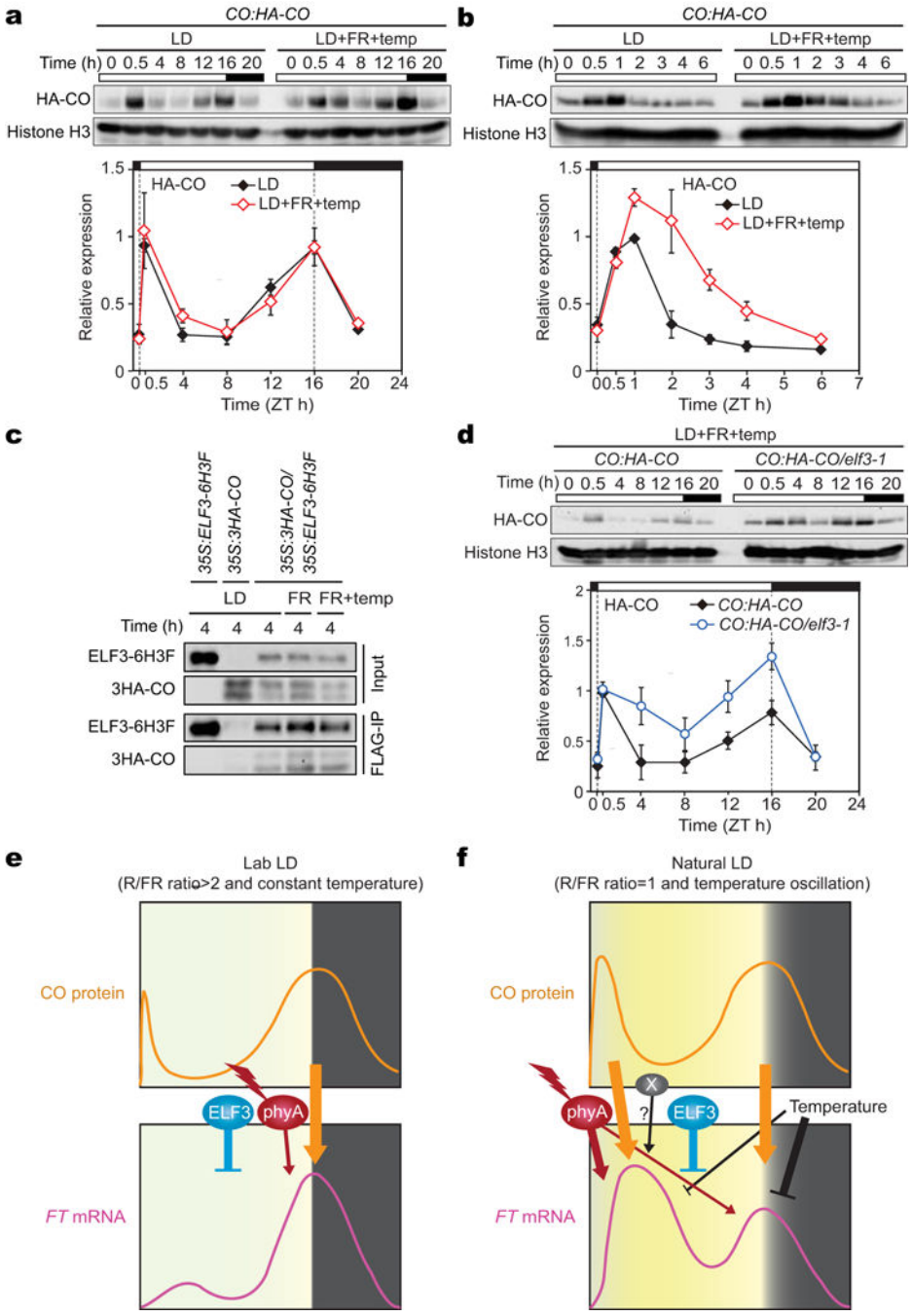

Fig. 5: CO protein stability was increased in LD+FR+temp during the morning.

a, **b**, CO protein accumulation patterns in *CO:HA-CO* plants in LD and LD+FR+temp. Histone H3 was used as a loading control. The quantification results represent means ± SEM [n=5 (**a**) and n=3 (**b**) biologically independent samples]. **c**, Coimmunoprecipitation analysis of ELF3 and CO proteins. *35S:ELF3–6H3F*, *35S:3HA-CO*, and *35S:3HA-CO/35S:ELF3–6H3F* plants were grown in LD, LD+FR (labeled as FR), or LD+FR+temp (FR+temp) and harvested in the morning (ZT4). The experiments were repeated three times independently, and similar results were obtained. **d**, CO protein accumulation patterns in *CO:HA-CO* and

CO:HA-CO/elf3–1 plants grown in LD+FR+temp. The quantification results represent means ± SEM (n=5 biologically independent samples). **e**, **f**, A model for CO-dependent *FT* regulation under natural LD conditions. This model shows temporal expression patterns of CO protein (top) and *FT* transcripts (bottom) under lab LD (**e**) and natural LD (**f**) conditions. **e**, Under artificial lab LD conditions in which the R/FR ratio is equal to or greater than 2 and the temperature is constant, CO protein appears to immediately accumulate after light onset and then rapidly degrade, resulting in low levels of CO protein in the morning and early afternoon. During this period, ELF3 protein inhibits *FT* expression through an unknown mechanism. CO protein peaks again at the end of the day, which directly activates *FT* transcription under these conditions. **f**, Under natural LD conditions, the R/FR ratio is 1 and the ambient temperature oscillates throughout the day. The amount of phyA protein increases in the morning, whereas the amount of ELF3 protein decreases (Fig. 3i, j). CO protein accumulates rapidly at high levels after sunrise, and CO protein degrades more slowly under natural LD conditions than under lab LD conditions. This CO accumulation might be important for morning induction of *FT*. In addition to the CO protein stability changes, there might be other factors (depicted as “X”) involved in the induction of morning *FT* under natural LD conditions. The phyA signal is positively involved in *FT* induction under these conditions. ELF3 negatively acts on *FT* regulation under these conditions. In addition, the temperature oscillations strongly repress *FT* transcription in the evening. Therefore, although CO protein abundance is high even at dusk, the levels of *FT* expression remain relatively low around dusk compared to morning. We showed that we can recreate these *FT* expression profiles in the lab by simply adjusting the R/FR ratio of light source and temperature conditions.